Measurements and Models for UWB Path Loss and Penetration Loss in Residential Environment

Monchai Chamchoy [1], Sathaporn Promwong [1], Suthichai Noppanakeepong [1], and J. Takada [2]
[1] *Faculty of Engineering, King Mongkut's Institute of Technology Ladkrabang*
Chalongkrung Rd., Ladkrabang, Bangkok 10520, Thailand, kcmoncha@kmitl.ac.th
[2] *Graduate School of Science and Engineering, Tokyo Institute of Technology*
2-12-1, O-okayama, Meguro-ku, 152-8552, Tokyo, Japan

Abstract

For the design of ultra wideband (UWB) communication, the characteristics of signal propagation are investigated. This paper contains measured data and empirical models for 3.1~10.6-GHz radio propagation path loss and aggregate penetration loss (APL) in residential areas for UWB applications. A frequency domain based experiment is performed for line-of-sight (LOS) and obstruction propagation conditions. The double ridged horn antenna and the biconical antenna are used to investigate the dependence of the antenna directivity on the UWB path loss. While the penetration loss is modeled under the directional propagation scheme. The characterization of the path loss exponent, n, and the APL are investigated. Therefore, the propagation prediction models are developed to understand the phenomenon of the futuristic indoor residential communication systems for home wireless networking.

1. INTRODUCTION

Recently, the U. S. Federal Communications Commission (FCC) allocated a very large portion of spectrum in the 3.1-10.6 GHz band for radio communication applications [1]. This spectrum is commonly called ultra wideband (UWB) with an effective isotropic radiated power (EIRP) below -41.3 dBm/MHz. The potential application of the UWB is to provide the wireless communications solutions for the indoor environment such as wireless personal area network (WPAN), home networking, and so on. Because of its low power spectral density and high data rate, the FCC has allowed UWB device to operate under the emission restriction and short range service area.

The focus of future home networking will be on the distribution of services. As the requirement for high data rate transmission of UWB system, the characteristics of path loss and penetration loss become an important role in the optimization of quality of service and coverage area. Numerous propagation studies show that the characteristics of path loss and penetration loss increase as the frequency increases. Especially, the impulse based UWB transmission scheme, information are transmitted by using an extremely short duration pulses with the pulse width of a sub-nanosecond, instead of continuous waves for narrowband communication. Because of the short duration of the pulse, the spectrum of the UWB signal can be several gigahertz wide. Pulse distortion due to the radio propagation channel, path loss and penetration loss are the keys to determine the system performance.

Several indoor residential environments have been studied extensively in literature [2]-[9]. Ghassemzadeh *et al.* showed how UWB path loss and time dispersion in home environments characterize in time and frequency domain. Additionally, an autoregressive model is developed for reconstruction of frequency domain channel response. However, most of these measurements are demonstrated for statistically path loss and time dispersion phenomenon such as delay spread. Unfortunately, the measurement bandwidth of some literatures much narrower than those for UWB band. Especially, there are no information on the aggregate penetration loss model for UWB communication. Moreover, the propagation characteristics of each sub-band system for multi-band UWB communication are differed. In this paper, the occupy bandwidth are considered for UWB path loss and penetration loss models in the residential environment.

The organization of the paper is as follows. Section II presents the measurement technique, hardware, and procedures. Section III details the methodology for path loss and penetration loss measurements and modeling. Section IV summarize the measurement results of the path loss and the penetration loss for each propagation condition. Section V discusses the data analysis for path loss exponent and path loss model with aggregate penetration loss. Section VI is conclusion.

2. DESCRIPTIONS OF MEASUREMENTS

The UWB channel characterizations can be achieved by performing measurements in time domain or in frequency domain. The real-time channel measurement can only be obtained in time domain. Unfortunately, noise, jitter, and synchronous are mainly degraded factors for channel measurement. On the other hand, when the network analyzer is used, the fundamental measurement limitation is the channel length. As we mentioned above, however, the UWB technology is proposed for the short-range wireless applications. Therefore, the frequency domain approach is the good candidate to measure the UWB channel in the residential environment.

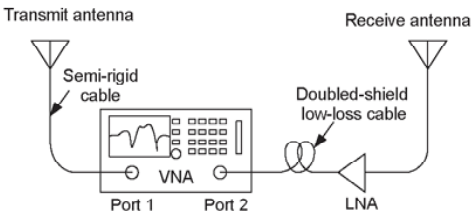

Fig. 1: Measurement setup.

A. Measurement Equipment

The vector network analyzer (VNA) is used as the frequency domain channel sounder in which the channel transfer function (CTF). Fig. 1 shows the configuration of the measurement setup for acquiring the complex frequency responses of the UWB channel via the S_{21} parameter. The VNA is set to sweep from 3 GHz to 7 GHz and 7 GHz to 11 GHz with each sub-band of 801 frequency tones. Therefore, the 1601 total frequency resolutions uniformly distributed over the 3-11 GHz band can be obtained. The laptop computer is used to control the VNA for recording the CTF. The transmit and receive antennas are connected to the VNA via the double-shielded low-loss cables, which extend the channel length up to 10 meters. The 30 dB ulta-wideband and low-noise amplifier is used to compensate the loss in the cables. Two kinds of the antennas are used to measure the UWB channel, namely, the double ridged horn (DRH) antenna and the biconical antenna, for representing the channel characterizations with the different antenna directivity. For all measurements, the antennas were vertically polarized. The limitation of the dynamic range for the VNA (HP 8510C) is exceeded 80 dB, including separation distance between antennas and cable losses.

B. Measurement Location

The measurements have been conducted in modern house in Bangkok, Thailand. Each room has the different size, layout and structure. Fig. 2 shows a simple layout of the building. The walls of the building are made of autoclaved aerated concrete internationally known as AAC, which is lighter than conventional ones. Several glass windows are used at the outside walls of the building. The ceilings are made of chipboard. The doors of the building and the furniture inside each room are made of wood.

The measurements were taken on first floor and second floor of the house. The room on the first floor is 10 m long, 8.5 m wide, and 2.5 m high. It was used to measure the propagation channel for the LOS scenario. Therefore, the transmitter (Tx) was placed at a fixed position, while the receiver (Rx) was moved throughout the room. On the second floor, the LOS propagation measurements were conducted in the bedroom A which has 10 m long, 6.5 m wide, and 2.5 m high. The bedroom B and C, 4 m long, 3.5 m wide, and 2.5 m high, were used to investigate the aggregate penetration loss by various obstruction materials. In this case, the Tx is placed at a fixed

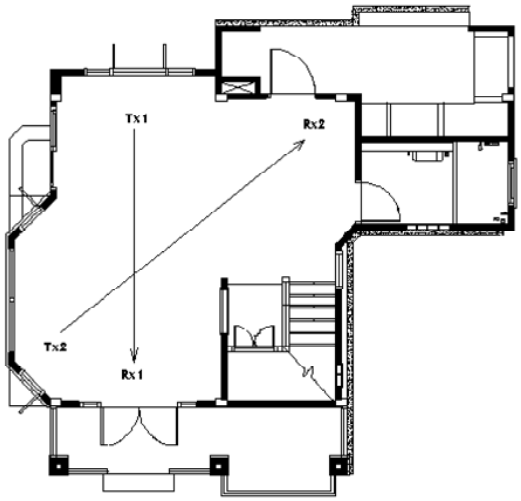

(a) First floor

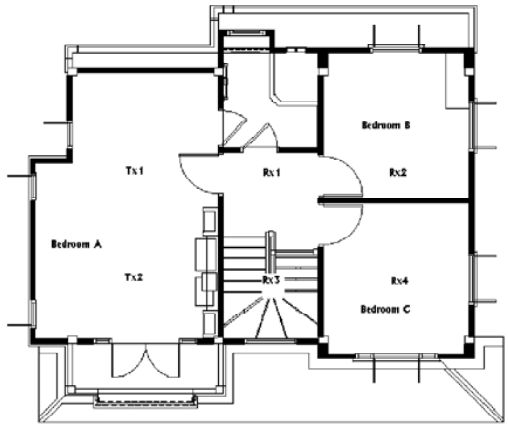

(b) Second floor

Fig. 2: Building layout.

position in the bedroom A, while the Rx was moved within the bedroom B and C, respectively.

C. Experiment Procedures

In order to keep the measurement channels as quasi-stationary, the surrounding environments are controlled to stationary, including human movement. The experiments are performed while the transmit antenna is located in a fixed position, and the receive antenna is moved within the house on the precisely measurement grids. The height of the transmit and receive antennas was fixed at about 1 meter for vertical polarizations. All measurements are made between 1 meter to 10 meters with intervals of 0.5 meter in the residential environment. In our experiment, the obstruction of the radio propagation by wood door, glass window, partition board, and concrete (AAC) wall are investigated for penetration loss model. For each measurement location for path loss modeling, the antenna

directivity are aligned and 32 snapshots are acquired by utilizing the computer controlled VNA, thus the noise can be canceled.

3. Definition of Path Loss and Penetration Loss

A. Path Loss Modeling

The path loss model is used to predict the radio coverage area between the transmitter and the receiver. The path loss exponent, n, is a measure of decay in signal power with distance, d, according to $1/d^n$. Therefore, the mean path loss is given by

$$\overline{PL}(d) \propto \left(\frac{d}{d_0}\right)^n \tag{1}$$

The path loss for any T-R separation distance is defined as

$$PL_{dB}(d) = PL_{dB}(d_0) + 10n\log_{10}\left(\frac{d}{d_0}\right) + X_\sigma;\ d > d_0 \tag{2}$$

where $PL_{dB}(d_0)$ is the average path loss at the reference distance, d_0 denotes the reference distance, $d_0 = 1$ m, n is the path loss exponent, and X_σ is a zero-mean log-normally random variable with standard deviation σ in decibels [10]. To model the path loss, the average path loss of the measured complex frequency response can be computed by

$$PL_{dB}(d) = 20\log_{10}\left[\frac{1}{MN}\sum_{i=1}^{N}\sum_{j=1}^{M}|H(f_i,x_j,d)|^2\right] \tag{3}$$

where $H(f_i,x_j,d)$ is the measured complex frequency response of the channel, N is the number of measured frequency tones and M is the number of snapshots over time at the distance d.

B. Definition of Penetration Loss

Aggregate penetration loss (APL) due to the building material is defined as the difference of the average received power between the measurement obtained before signal transmitted to the building material and the average received power measured after signal propagated through the building material for a constant transmitter location. The relationship of the aggregate penetration loss can therefore be written as [11]

$$APL\ [dB] = 10\log_{10}\left[\frac{\frac{1}{MN}\sum_{i=1}^{N}\sum_{j=1}^{M}P(f_i,x_j)^{(\text{before})}}{\frac{1}{MN}\sum_{j=1}^{N}\sum_{i=1}^{M}P(f_i,x_j)^{(\text{after})}}\right]. \tag{4}$$

The summation of (4) is over the N number of measured frequency tones and M number of snapshots over time, each denoted as $P(f_i,x_i)$. All powers are in absolute power scale (not dB values).

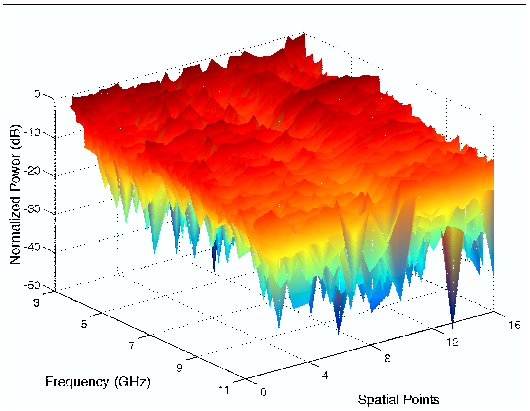

(a) omnidirection-omnidirection

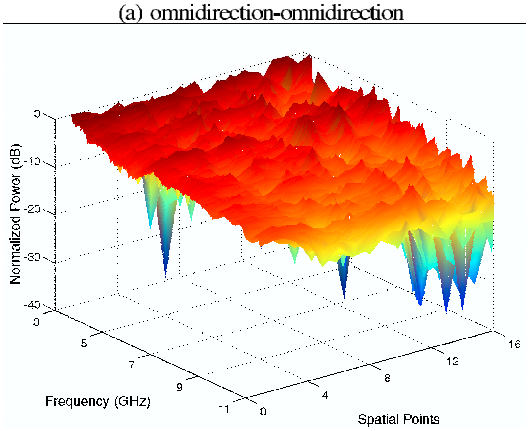

(b) direction-omnidirection

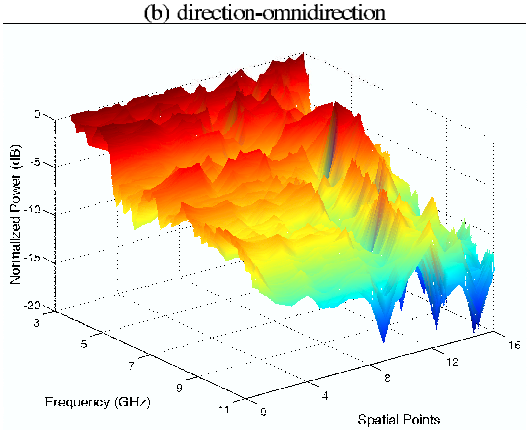

(c) direction-direction

Fig. 3: Normalized 3-D channel transfer function at several spatial points.

4. Measurement Results

Based on the swept frequency measurement by using the VNA, the complex frequency responses of the in-home UWB channels are measured over the frequency range of 3 GHz to 11 GHz. To obtain the path loss exponent of the measured channel as described in equation (2), the minimum mean square error (MMSE) fitting method is used to estimate n for all the indoor measurements at the residential environment. The log-normal

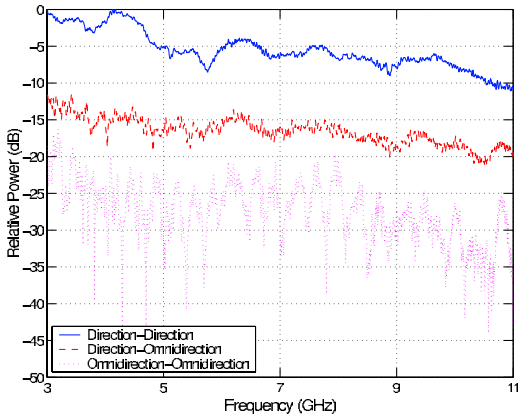

Fig. 4: Time-average normalized 2-D channel transfer function at a spatial point of 1 meter T-R separation distance.

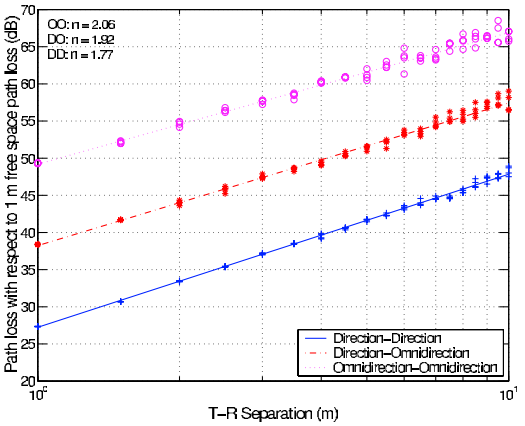

Fig. 5: Time-average path loss for all the antenna directivity measurement data.

standard deviation, σ, is modeled by computing the deviation of the obtained fitting data. Fig. 3 illustrated the normalized 3-D channel transfer function for each propagation scheme at several spatial points over the 32 time-snapshots. The corresponding time-average normalized 2-D channel transfer function for all propagation conditions, namely, direction-direction, direction-omnidirection, and omnidirection-omnidirection, is shown in Fig. 4, respectively.

Fig. 5 shows the scatter plot of the path loss as the function of the T-R separation distance for all antenna directivity in the LOS environment. The path loss exponent, n, is found to be 1.77, 1.92, and 2.06 for measurement with direction-direction, direction-omnidirection, and omnidirection-omnidirection propagation schemes, respectively, for full band UWB communication. The standard deviations are 1.64, 1.35, and 0.82, respectively, We can observed the logarithmic description of the energy versus the T-R separation distance. From these figures, it can be note that the deviation of the path loss can be described by the log-normal shadowing. The path loss exponent, n, the standard deviation, σ, and free space path loss, $PL(d_0)$, are listed for each propagation condition in Table 1.

The scatter plots of the path loss as the function of the T-R separation distance for each antenna directivity in the LOS environments are shown in Fig. 6. Unlike the full band communication, the path loss exponents for the multi-band propagation can change variously, according to each antenna directivity and frequency band. For example, the path loss exponent of the omnidirection to the omnidirection propagation is randomly varied between 1.52 and 2.12. However, the path loss at the reference distance, $d = 1$ m, is quite depends upon the subband frequency. In addition, the reference path loss also depends on the antenna directivity. The path loss exponent (n) and the reference path loss for the multi-band communication channel are listed for each propagation conditions in Table 2.

Based on the measurement data, the general propagation prediction method is the path loss exponent model, given in (2). The model only requires know of the T-R separation distance, the reference path loss and standard deviation as given in Table 1 for full band propagation while the characteristics of the multi-band path loss are shown in Table 2. The actual path loss tends to be log-normally distributed around the predicted path loss as shown in Fig. 5 and Fig. 6 for the full band and the multi-band propagation channel, respectively.

TABLE 1: SUMMARY OF PATH LOSS EXPONENTS FOR VARIOUS ANTENNA DIRECTIVITY IN LOS CONDITION.

Propagation Condition	$PL(d_0)$ (dB)	n	σ (dB)
Direction-Direction	27.24	1.77	1.64
Direction-Omnidirection	38.23	1.92	1.35
Omnidirection-Omnidirection	49.19	2.06	0.82

Table 3 shows all of the aggregate penetration loss values and material thickness for residential propagation studied. The aggregate penetration loss is found to be 1.61, 1.92, 2.22, and 13.92 dB for propagation obstruction by glass, dry wood, partition board, and concrete (AAC), respectively.

5. DATA ANALYSIS

In this section, the general analysis of the measured path loss data is presented. This includes the path loss exponent models for different antenna directivity and aggregate penetration loss by various obstruction materials.

A. Path Loss Exponent Models

Based on the measurement data, the general propagation prediction method is the path loss exponent model, given in (2). The model only requires knowledge of the T-R separation distance, free space path loss and standard deviation as given in Table 1. The actual path loss tends to be log-normally distributed around the predicted path loss as shown in Fig. 5.

B. Path Loss Models With Aggregate Penetration Loss

Modeling of path loss with aggregate penetration loss is one of the most critical aspects to estimate the received signal power for the through-wall propagation. In this model, the path loss exponent, n, is used to predict the received signal

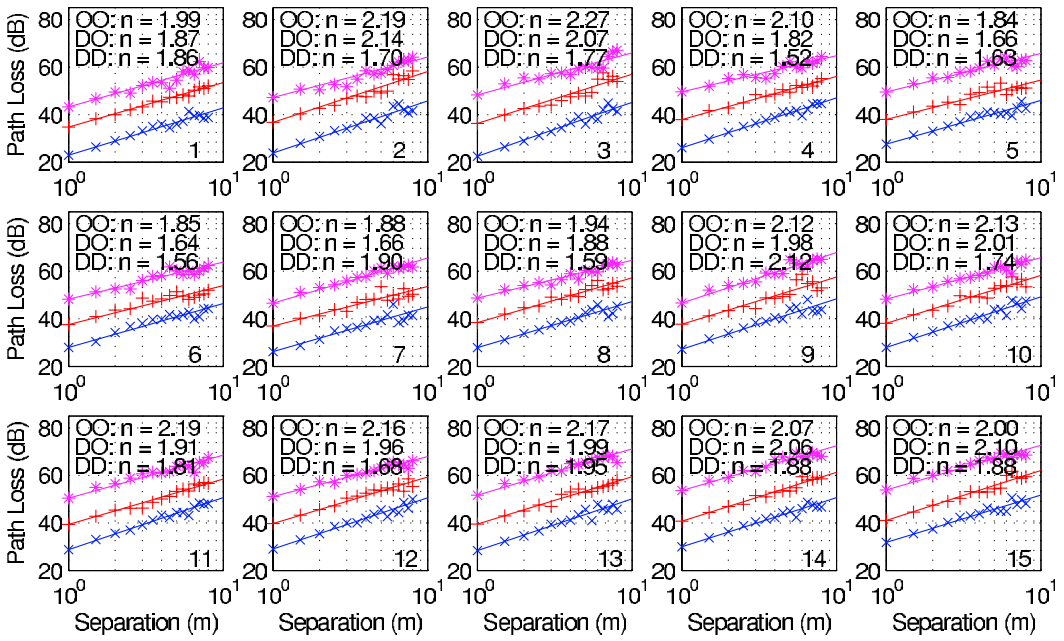

Fig. 6: Scatter plots of the measurement path loss and the modeled path loss for the multi-band UWB propagation channel. The upper line, the middle line and the lower line represent the propagation condition for the direction-direction, the direction-omnidirection and the omnidirection-omnidirection channel, respectively.

TABLE 2: SUMMARY OF PATH LOSS EXPONENTS n, AND $PL(d_0)$ FOR MULTI-BAND UWB PROPAGATION.

Subband	Dir-Dir		Dir-Omni		Omni-Omni	
	$PL(d_0)$	n	$PL(d_0)$	n	$PL(d_0)$	n
1	22.94	1.86	34.80	1.87	43.22	1.99
2	23.86	1.70	36.77	2.14	47.23	2.19
3	22.50	1.77	36.31	2.07	48.31	2.27
4	26.07	1.52	37.91	1.82	49.61	2.10
5	27.58	1.63	37.97	1.66	49.49	1.84
6	27.94	1.56	37.59	1.64	48.25	1.85
7	26.20	1.90	37.01	1.66	46.55	1.88
8	27.87	1.59	38.44	1.88	48.70	1.94
9	27.23	2.12	37.75	1.98	46.68	2.12
10	27.94	1.74	38.13	2.01	48.28	2.13
11	28.78	1.81	39.37	1.91	50.44	2.19
12	29.02	1.68	39.73	1.96	51.10	2.16
13	28.40	1.95	39.54	1.99	51.66	2.17
14	29.93	1.88	40.71	2.06	53.63	2.07
15	31.77	1.88	41.07	2.10	53.88	2.00

TABLE 3: AGGREGATE PENETRATION LOSS (APL) VALUES FOR ALL OBSTRUCTION MATERIALS USING DIRECTION-DIRECTION PROPAGATION MEASUREMENT.

Material	Thickness	APL (dB)
Glass	1.0 cm.	1.61
Dry Wood	3.5 cm.	1.92
Partition Board	6.0 cm	2.22
Concrete (AAC)	12.0 cm	13.92

power before obstruction. The aggregate penetration loss is added to the model of propagation path loss as

$$PL(d) = PL(d_0) + 10n\log_{10}\left(\frac{d}{d_0}\right) + APL + X_\sigma. \quad (5)$$

The aggregate penetration loss is chosen from Table 3 based on the building material.

Fig. 7 shows the comparison of the path loss exponent model with aggregate penetration loss and the measured path loss for radio wave obstructing by concrete (AAC). It is found that the model is close to the measurement data.

6. CONCLUSIONS

This paper has presented the results of path loss exponent and aggregate penetration loss for UWB communication in residential environment. The measurements were performed in the 3 GHz to 11 GHz band for the various antenna configurations, namely, direction-direction, direction-omnidirection, and ominidirection-omnidirection propagation. The path loss increases as the T-R separation distance increases. For free space propagation, n equals 2. As the empirical models, the path loss exponent can be changed between 1.77 to 2.06, depending on the antenna directivity. This work also determined how building material influence the penetration of radio propagation for home wireless networking. The results show that, the aggregate penetration loss can be increased from 1.61 dB to 13.92 dB, depending on the building material.

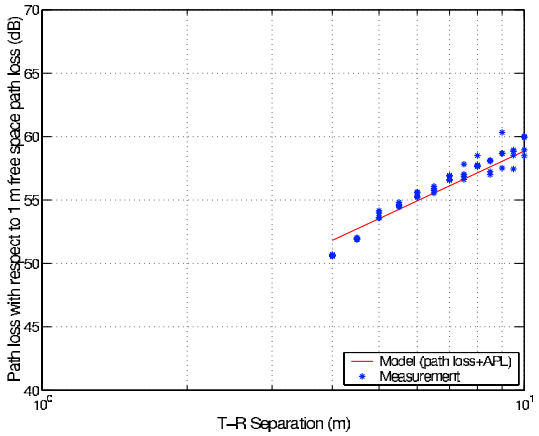

Fig. 7: Path loss exponent model with aggregate penetration loss and the measured path loss for radio wave obstructing by concrete (AAC).

REFERENCES

[1] Federal Communications Commission, First order and report: Revision of part 15 of the Commission's rules regarding UWB transmission systems, Apr. 22, 2002.

[2] S. S. Ghassemzadeh, L. J. Greenstein, A. Kavcic, T. Sveinsson, and V. Tarokh, "UWB indoor path loss model for residential and commercial buildings," in *Proc. IEEE Vehicular Technology Conf. Fall 2003*, pp. 629-633, 2003.

[3] S. S. Ghassemzadeh, L. J. Greenstein, A. Kavcic, T. Sveinsson, and V. Tarokh, "UWB indoor delay profile model for residential and commercial environments," in *Proc. IEEE Vehicular Technology Conf. Fall 2003*, pp. 3120-3125, 2003.

[4] S. S. Ghassemzadeh, R. Jana, C. W. Rice, W. Turin, and V. Tarokh, "Measurement and modeling of an ultra-wide bandwidth indoor channel," *IEEE Trans. Commun.*, Vol. 52, pp. 1786-1796, Oct. 2004.

[5] Y. Suzuki and T. Kobayashi, "Ultra wideband signal propagation in desktop environments," *IEEE UWBST2003*, pp. 493-497, 2003.

[6] R. M. Buehrer, W. Davis, A. Safaai-Jazi, and D. Sweeney, "Characterization of the Ultra-wideband Channel," *IEEE UWBST2003*, 2003.

[7] S. S. Ghassemzadeh, L. J. Greenstein, T. Sveinsson, A. Kavcic, and V. Tarokh, "UWB delay profile models for residential and commercial indoor environments," *IEEE Trans. Vehicular Technology*, Vol. 54, No. 4, pp. 1235-1244, July 2005.

[8] C.-C. Chong and S. K. Yong, "A generic statistical-based UWB channel model for high-rise apartments," *IEEE Trans. Antennas and Propag.*, Vol. 53, No. 8, pp. 2389-2399, August 2005.

[9] Q. Li and W. S. Wong, "Measurement and analysis of the indoor UWB channel," in *Proc. IEEE Vehicular Technology Conf. Fall 2003*, Vol. 1, pp. 1-5, 2003.

[10] T. S. Rappaport, *Wireless Communications: Principles and Practice*, Prentice Hall PTR, Upper Saddle River, NJ, USA, 2nd edition, 2002.

[11] S. Aguirre, L. H. Loew, and L. Yeh, "Radio propagation into buildings at 912, 1920, and 5990 MHz using microcells," in *Proc. 3rd IEEE ICUPC*, Oct. pp. 129-134, 1994.